

Thermal Decomposition Kinetics and Structure of Novel Polystyrene Clusters with MTEMPO as a Branching Agent

Aizhen Niu,[†] Chengming Li,[‡] Yue Zhao,^{†,§} Junpo He,[‡] Yuliang Yang,^{*,‡} and Chi Wu^{*,†,§}

The Open Laboratory of Bond Selective Chemistry, Department of Chemical Physics, University of Science and Technology of China, Hefei, Anhui, China; Department of Chemistry, The Chinese University of Hong Kong, Shatin, N. T., Hong Kong; and Department of Macromolecular Science, Fudan University, The Open Laboratory of Macromolecular Engineering, State Commission of Education, Shanghai, China

Received March 30, 2000; Revised Manuscript Received November 15, 2000

ABSTRACT: Polystyrene clusters were prepared by using a trace amount of 4-methacryloyloxy-2,2,6,6-tetramethylpiperidine-1-oxy (MTEMPO) as a branching agent. Such clusters can undergo a thermal decomposition into linear chains at temperatures higher than 100 °C. The thermal decomposition was studied by a combination of static and dynamic laser light scattering (LLS). The time dependence of the weight-average molar mass (M_w), the root-mean-square z -average radius of gyration ($\langle R_g^2 \rangle_z^{1/2}$), and the average hydrodynamic radius ($\langle R_h \rangle$) was used to monitor the decomposition kinetics and cluster structure. It has been found that $M_w \propto t^{-\alpha}$, and the decomposition can be roughly divided into three stages; namely, from large clusters to smaller ones; from smaller clusters to less-branched ones; and finally to short linear chains. The scaling of $\langle R_g \rangle \propto M_w^{0.33 \pm 0.01}$ in the first stage indicates that these clusters are uniform in density, which is rare and much different from conventional polymer clusters whose density decreases from center to periphery. Moreover, we observed, for the first time, that $\langle R_g \rangle / \langle R_h \rangle \propto M_w^{-0.20 \pm 0.01}$, revealing that even for a uniform cluster swollen in a good solvent, its periphery is still more hydrodynamically draining.

Introduction

Polymers with special architectures, such as star, block, grafting, and hyperbranching, often display unusual properties. They can be prepared by different polymerization methods.^{1–3} Recently, controlled radical polymerization was developed, in which a stable radical, such as TEMPO (2,2,6,6-tetramethylpiperidine-1-oxy), could reversibly couple with a growing radical.^{4–7} Using this method, a number of polymers with controlled architectures were synthesized.^{8–12} In a previous study, a controlled radical polymerization in the presence of a polymerizable nitroxide, 4-methacryloyloxy-2,2,6,6-tetramethylpiperidine-1-oxy (MTEMPO), was investigated.¹³ The initial purpose was to enhance the polymerization rate, assuming that the polymerized MTEMPO would be more bulky and less active in trapping growing radicals. However, the polymerization turned out to be less controllable, reflecting in an unexpected increase of molar mass and a higher polydispersity. On the basis of a primary structural analysis, we proposed a thermally reversible branched structure because each C–ON linkage acted as a branching point.

Note that the formation of branched structure has been extensively studied.^{14,15} It is now generally accepted that there are two limiting regimes: (i) the diffusion-limited cluster aggregation (DLCA), in which each collision between two clusters results in the formation of a permanent bond; and (ii) the reaction-limited cluster aggregation (RLCA), in which only a small fraction of intercluster collisions leads to the formation of a bond. The concept of fractal has been used

to characterize the structure of such a disordered system. For fractal structures, mass (M) is related to size (R) via a well-known scaling, $M \propto R^D$, where D is the fractal or Hausdorff dimension. Depending on the formation process,¹⁶ D ranges from 1.78 to 2.10, which is lower than a normal spatial dimension of $d = 3$ because of a nonuniform density, decreasing from center to periphery.¹⁷ Nakata et al.¹⁸ recently reported that the aggregation of poly(methyl methacrylate) in isoamyl acetate led to a much higher fractal dimension of $D = 2.86 \pm 0.03$.

To our knowledge, the decomposition of polymeric clusters have not been seriously studied, partially attributed to the fact that such polymeric clusters are rare. In this study, we prepared novel polystyrene clusters with MTEMPO as a branching agent. Each MTEMPO branching point can undergo a thermally reversible decomposition. The thermal decomposition kinetics and structure of these clusters in toluene at elevated temperature were investigated by using a combination of static and dynamic laser light scattering.

Experimental Section

Sample Preparation. The synthesis of methacrylate tetramethylpiperidinyloxy (MTEMPO) modified polystyrene involved two steps. The first was to prepare stable and polymerizable nitroxyl radical MTEMPO by Scheme 1.¹⁹ A solution of 20 g (0.23 mol) of freshly distilled methacrylic acid, 0.44 mol of freshly distilled benzoyl chloride, and 1.1 g of hydroquinone was refluxed at 140 °C for half an hour. The distillation of such a solution mixture resulted in 18.4 g of methacryl chloride. Into one solution mixture of 10 g (0.058 mol) of HTEMPO, 7.1 g (0.07 mol) of Et₃N, and 200 mL of dry benzene, another solution mixture of 7.4 g (0.07 mol) of methacryl chloride and 20 mL of dry benzene was added dropwise under vigorous stirring at room temperature. In this two-solution mixture, methacryl chloride was reacted with

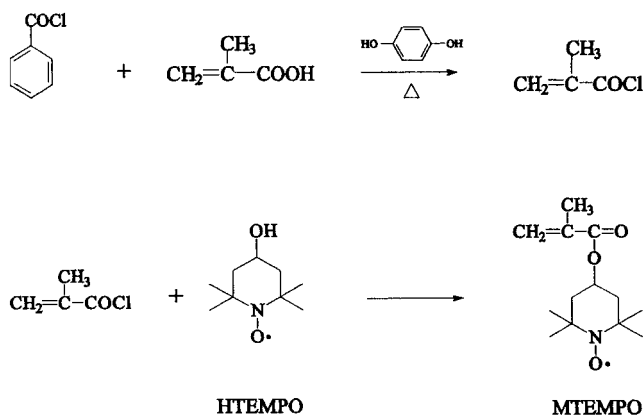
[†] The Chinese University of Hong Kong.

[‡] Fudan University.

[§] University of Science and Technology of China.

* To whom correspondence should be addressed.

Scheme 1. Synthesis of Stable and Polymerizable Nitroxyl Radical



HTEMPO at room temperature for 1 h and then at 70 °C for 2 h. The precipitate was removed by filtration. The orange crude product obtained by evaporation was further purified by recrystallization in cyclohexane. The resultant orange crystal had a melting point in the range 82.2–84.0 °C. The total yield of the reaction was 7.2 g (51.8%).

The second step was to synthesize MTEMPO modified polystyrene. A solution mixture of 41.6 g (0.4 mol) of freshly distilled styrene, 0.290 g (1.2 mmol) of benzoyl peroxide as initiator, and 0.288 g (1.2 mmol) of MTEMPO first undergone two freeze–thaw cycles in liquid nitrogen and then was heated to 120 °C to start the polymerization. After a 28 h reaction under nitrogen atmosphere, the reaction mixture was quenched into liquid nitrogen to stop the polymerization. The mixture was dissolved in toluene and precipitated in methanol. The polystyrene precipitate separated by filtration was dried in a vacuum at 50 °C. The O–C bond between nitroxide and polystyrene can undergo a reversible dissociation at ~100 °C so that each MTEMPO unit can form a thermally reversible branching point,²⁰ as shown in Scheme 2. Note that MTEMPO is so small that its size is insignificant in comparison with individual polymer chains. In this study, ascorbic acid was

added to trap the resultant free radicals and make the dissociation irreversible so that we can study the cluster structure at each stage of the decomposition. The molar ratio of ascorbic acid to alkoxyamine was ~3. The decomposition was conducted at 100 and 110 °C under stirring. A small portion of the solution was removed and cooled at different decomposition times.

Laser Light Scattering. The details of LLS instrumentation can be found elsewhere.^{21,22} A commercial LLS spectrometer (ALV/SP-150 equipped with an ALV-5000 digital time correlator and an ADLAS DPY425II solid-state laser as the light source, output power = 400 mW at $\lambda_0 = 532$ nm) was used. The solutions were clarified with a 0.22 μm Millipore filter to remove dust. In static LLS, the angular dependence of the excess absolute time-average scattered intensity, known as the Rayleigh ratio $R_{v\nu}(q)$, of a dilute polymer solution at concentration C (g/mL) and the scattering angle θ was measured. $R_{v\nu}(q)$ is related to the weight-average molar mass M_w , the root-mean-square radius of gyration $\langle R_g^2 \rangle^{1/2}$ (or written as $\langle R_g \rangle$), and polymer concentration C as^{23,24}

$$\frac{KC}{R_{v\nu}(q)} \cong \frac{1}{M_w} \left(1 + \frac{1}{3} \langle R_g^2 \rangle q^2 \right) + 2A_2 C \quad (1)$$

where $K = 4\pi^2 n^2 (dn/dC)^2 / N_A \lambda_0^4$ and $q = (4\pi n / \lambda_0) \sin(\theta/2)$ with N_A , dn/dC , n , λ_0 , and θ being the Avogadro number, the specific refractive index increment, the solvent refractive index, the wavelength of light in vacuo, and the scattering angle, respectively. A_2 is the second virial coefficient.

In dynamic LLS, an intensity–intensity time correlation function $G^{(2)}(t, q)$ in the self-beating mode can be measured, which can be expressed as^{23,24}

$$G^{(2)}(t, q) = \langle I(t, q) I(0, q) \rangle = A [1 + \beta |g^{(1)}(t, q)|^2] \quad (2)$$

where A is a measured baseline; β , a parameter depending on the detection optics; t , the delay time; $q = (4\pi n / \lambda_0) \sin(\theta/2)$ with n , λ_0 , and θ being the solvent refractive index, the wavelength of the laser light in a vacuum and the scattering angle, respectively; and $g^{(1)}(t, q)$, the normalized first-order electric field time correlation function. For a polydisperse sample, $g^{(1)}$

Scheme 2. Thermally Reversible and Irreversible Decomposition of MTEMPO Modified Polystyrene

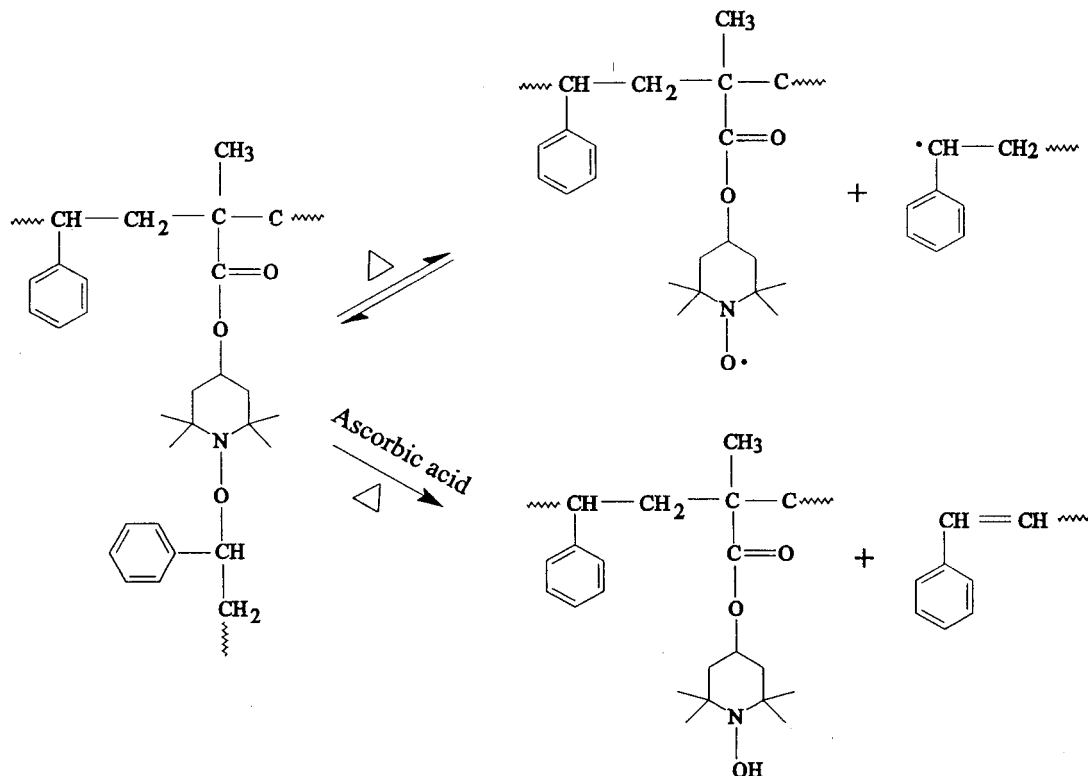
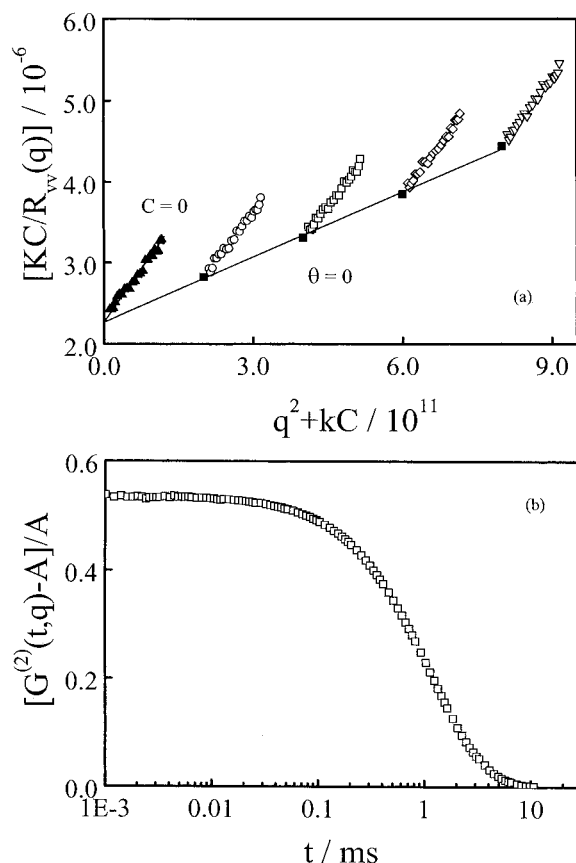


Table 1. Light-Scattering Characterization of Three MTEMPO (4-Methacryloyloxy-2,2,6,6-tetramethylpiperidine-1-oxyl) Modified Polystyrene Clusters in Toluene at 25 °C

sample	MTEMPO styrene (mol %)	initiator (mol %)	$M_w \times 10^{-5}$ (g/mol)	$\langle R_g \rangle$ (nm)	$\langle R_h \rangle$ (nm)	$\langle R_g \rangle / \langle R_h \rangle$	M_w / M_n
1	0.15	0.3	1.66 ± 0.02	15.8 ± 0.5	12.6 ± 0.1	1.25	1.52
2	0.3	0.3	5.48 ± 0.02	25.8 ± 0.5	22.1 ± 0.1	1.17	1.56
3	0.6	0.3	4.81 ± 0.02	23.4 ± 0.5	20.2 ± 0.1	1.16	1.60

**Figure 1.** (a) Typical Zimm plot of MTEMPO modified polystyrene cluster (sample 3) in toluene, where $T = 25.0$ °C and C ranges from 5×10^{-4} to 4.01×10^{-3} g/mL. (b) Typical measured intensity–intensity time correlation function $G^{(2)}(t, q)$ for MTEMPO modified polystyrene cluster (sample 3) in toluene at $\theta = 15^\circ$.

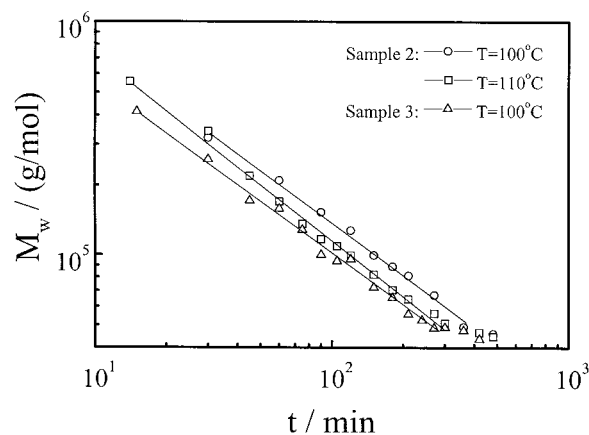
(t, q) is related to the line-width distribution $G(\Gamma)$ by^{23,24}

$$g^{(1)}(t, q) = \langle E(t, q) E(0, q) \rangle = \int_0^\infty G(\Gamma) \exp(-\Gamma t) d\Gamma \quad (3)$$

Γ is a characteristic line width. For a pure diffusion relaxation, Γ can be related to the translational diffusion coefficient D by $\Gamma = Dq^2$. $G(\Gamma)$ can be calculated from the Laplace inversion. The well-accepted Laplace inversion CONTIN algorithm was used in this study.²⁵ D can be further related to the hydrodynamic radius R_h by $R_h = k_B T / (6\pi\eta D)$, where k_B and η are the Boltzmann constant and solvent viscosity, respectively.

Results and Discussion

Figure 1 shows a typical Zimm plot and a typical measured intensity–intensity–time correlation function. On the basis of eq 1, $\langle R_g \rangle$, A_2 , and M_w can be calculated from the slopes of $[KC/R_{vv}(q)]_{C \rightarrow 0}$ vs q^2 and $[KC/R_{vv}(q)]_{q \rightarrow 0}$ vs C and the intercept of $[KC/R_{vv}(q)]_{C \rightarrow 0, q \rightarrow 0}$, respectively. Table 1 summarizes LLS characterization of the three samples prepared with different initial MTEMPO/styrene ratios. Sample 1 has a lower M_w than samples 2 and 3 because a less amount of MTEMPO (“branching agent”) was used. The ratio of

**Figure 2.** Decomposition time dependence of weight-average molar mass (M_w) of MTEMPO modified polystyrene clusters.

$\langle R_g \rangle / \langle R_h \rangle$ reflects the structure or conformation.²⁶ For example, for uniform and nondraining spheres, $\langle R_g \rangle / \langle R_h \rangle \sim 0.774$; for hyperbranched polymer clusters, $\langle R_g \rangle / \langle R_h \rangle \sim 1.0$ – 1.3 , depending on the branching degree; and for flexible random coil chains, $\langle R_g \rangle / \langle R_h \rangle \sim 1.5$ – 1.8 , depending on the chain polydispersity. The decrease of $\langle R_g \rangle / \langle R_h \rangle$ as the MTEMPO content increases indicates that sample 1 is less branching.

Figure 2 shows that, during the decomposition, the weight-average molar mass (M_w) of the clusters decreases as time (t) increases, in which M_w could be scaled to t by $M_w \propto t^{-\alpha}$, α is a scaling constant, characterizes the decomposition time dependence of M_w . For sample 2 at 100 and 110 °C, $\alpha = 0.74 \pm 0.01$ and $\alpha = 0.80 \pm 0.01$, respectively, indicating that the decomposition rate slightly increases as the temperature increases. On the other hand, for a given temperature, there is nearly no difference in the decomposition rate between samples 2 and 3. Our results showed that for the different samples the decomposition led to similar linear polystyrene chains with a weight-average molar mass close to 4×10^4 g/mol. On the basis of the initial MTEMPO/styrene ratios listed in Table 1, we estimate that on average each polystyrene chain in samples 1, 2, and 3 contains ~ 2 – 3 , 17, and 29 MTEMPO groups, respectively. Our results indicate that samples 2 and 3 have a similar branching degree, which does not increase as the MTEMPO/styrene ratio increases when the concentration of MTEMPO is higher than that of the initiator (benzoyl peroxide).

Figure 3 shows that during the decomposition there is no significant change in the polydispersity (M_w/M_n) except a slight decrease after $t > \sim 300$ min, where M_n is the number-average molar mass. This indicates that the MTEMPO branching points are randomly cleaved or decomposed; in other words, the cleavage has no preference in the periphery or the center of the cluster. M_w/M_n was estimated from the relative width ($\mu_2/\langle \Gamma \rangle^2$) of the line-width distribution $G(\Gamma)$ obtained in dynamic laser light scattering by using $M_w/M_n \sim 1 + 4\mu_2/\langle \Gamma \rangle^2$, where μ_2 is defined as $\int G(\Gamma)(\Gamma - \langle \Gamma \rangle)^2 d\Gamma$. The final value of $M_w/M_n \sim 1.4$ shows that the resultant linear chains

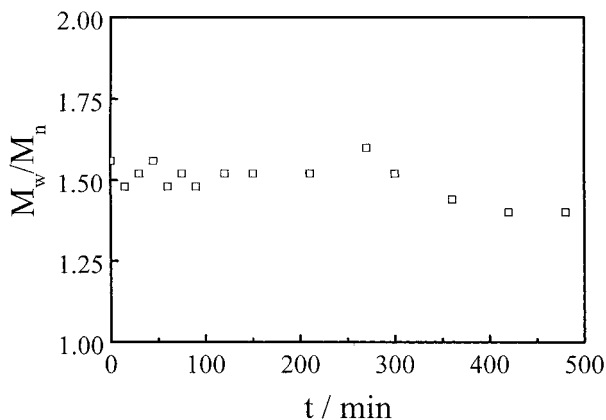


Figure 3. Typical decomposition time dependence of polydispersity index (M_w/M_n) of sample 2, where M_w/M_n was estimated from relative width of line-width distribution obtained in dynamic laser light scattering. The estimation agrees with results from gel permeation chromatography (GPC).

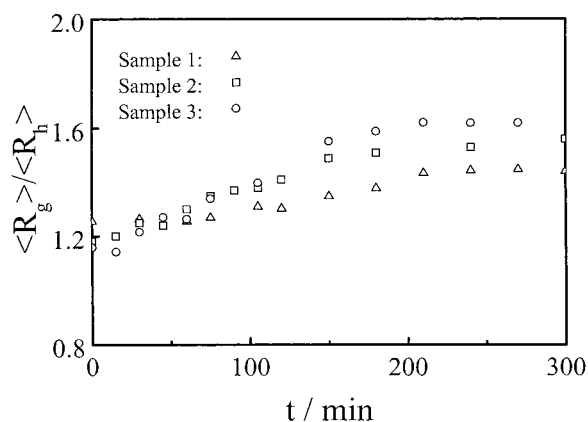


Figure 4. Typical decomposition time dependence of ratio of average radius of gyration to average hydrodynamic radius ($\langle R_g \rangle / \langle R_h \rangle$) of MTEMPO modified polystyrene clusters in toluene at 100 °C.

have a relatively narrow distribution in molar mass, revealing the “living” nature of the polymerization.

The conformation change during the decomposition can be better viewed in the terms of $\langle R_g \rangle / \langle R_h \rangle$. Figure 4 shows a linear increase of $\langle R_g \rangle / \langle R_h \rangle$ as the decomposition time increases in the range ~ 60 – 200 min, revealing that larger hyperbranched clusters were gradually broken down into smaller less-branched clusters and eventually into linear chains. Figure 4 shows that, in both time ranges $t < 60$ min and $t > 200$ min, $\langle R_g \rangle$ decreases as t increases, but $\langle R_g \rangle / \langle R_h \rangle$ remains a constant. This suggests that, in the range of $t < 60$ min, large clusters evenly break into smaller ones and the hyperbranched structure remains, while in the range of $t > 200$ min, long linear chains made of short linear polystyrene chains via the MTEMPO connection are cleaved into short linear ones. Therefore, the decomposition contains three different stages, as schematically shown in Figure 5.

Figure 6 shows that for three different samples the double-logarithmic plots of $\langle R_g \rangle$ vs M_w collapsed into a single one. In the higher molar mass range, $\langle R_g \rangle$ can be scaled to M_w by $\langle R_g \rangle \propto M_w^{0.33 \pm 0.01}$, indicating that the density of the clusters is uniform; in other words, there is no chain density distribution from the center to the periphery of the clusters, which is rare for polymer clusters. It should be stated that, using molecular dynamic simulations, Grest et al.²⁷ found that dendrim-

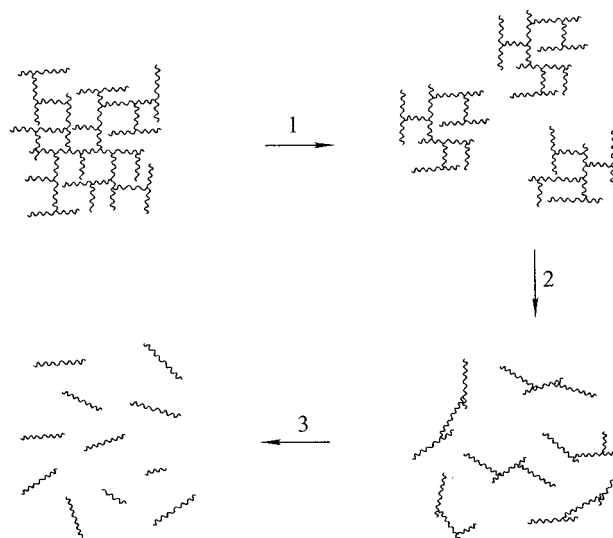


Figure 5. Schematic of a three-stage thermal decomposition of TEMPO modified polystyrene clusters in toluene at high temperatures.

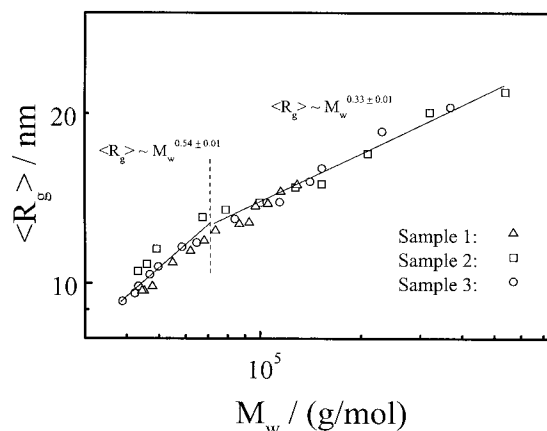


Figure 6. Double-logarithmic plot of average radius of gyration ($\langle R_g \rangle$) vs weight-average molar mass (M_w) of MTEMPO modified polystyrene clusters during thermal decomposition at 100 °C.

ers have a compact (space filling) structure and uniform density, so that their radius of gyration can also be scaled to the molar mass as $R_g \propto M^{1/3}$. In the low molar mass range, $\langle R_g \rangle \propto M_w^{0.54 \pm 0.01}$, representing a typical behavior of linear polymer chains in good solvent. A combination of the slope difference in the low and high molar mass ranges in Figure 6 and the variation of $\langle R_g \rangle / \langle R_h \rangle$ in Figure 4 indicates that the initial decomposition was dominated by a cluster-to-cluster process while the final stage of the decomposition involved a cluster-to-linear chain process.

Figure 7 shows that for three different samples studied the average translational diffusion coefficient ($\langle D \rangle$), a hydrodynamic property, can be also scaled to M_w by $\langle D \rangle \sim M_w^{-\alpha_D}$ with $\alpha_D = 0.53 \pm 0.01$, where α_D is a scaling constant. Note that $\langle D \rangle$ measures the cluster's hydrodynamics in solution and is related to the average hydrodynamic radius ($\langle R_h \rangle$) via the Stokes–Einstein equation $R_h = k_B T / (6\pi\eta D)$ where k_B , η , and T is the Boltzmann constant, solvent viscosity, and the absolute temperature, respectively. If the conformation is independent of the chain length, α should close to α_D . A combination of Figures 6 and 7 shows that $\langle R_g \rangle / \langle R_h \rangle \propto M_w^{-0.20 \pm 0.01}$ in the high molar mass range; i.e., $\langle R_g \rangle /$

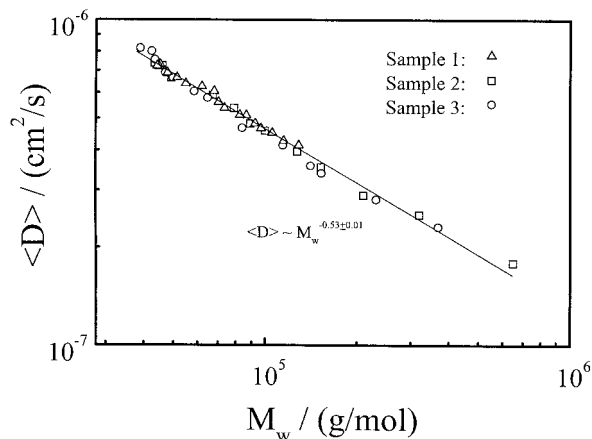


Figure 7. Double-logarithmic plot of average translational diffusion coefficient $\langle D \rangle$ vs weight-average molar mass (M_w) of MTEMPO modified polystyrene clusters during thermal decomposition at 100 °C.

$\langle R_h \rangle$ increases as M_w decreases. This is because decrease of $\langle R_h \rangle$ with M_w is faster than that of $\langle R_g \rangle$. Note that $\langle R_g \rangle / \langle R_h \rangle$ is often used to estimate the chain conformation or the density distribution. However, we have to rethink the linkage between the chain conformation and $\langle R_g \rangle / \langle R_h \rangle$ because in the first decomposition stage the clusters studied are uniform, and their structure is independent of molar mass. The molar mass dependence of $\langle R_g \rangle / \langle R_h \rangle$ clearly tells us that even for a uniform polymer cluster swollen in a good solvent, its periphery is more hydrodynamically draining than its center; i.e., the solvent molecules in the center are less mobile. As its molar mass decreases, the draining periphery contributes more and more to $\langle R_h \rangle$ so that the decrease of $\langle R_h \rangle$ with M_w is faster than that of $\langle R_g \rangle$. Weill and des Cloizeaux²⁸ showed that for long linear polymer chains in good solvents $\langle R_g \rangle / \langle R_h \rangle \sim M^{0.05 \pm 0.02}$; i.e., the ratio increases with M , because the hydrodynamic properties converge much more slowly to the asymptotic limit ($N \rightarrow \infty$) than the static properties. To our knowledge, the decrease of $\langle R_g \rangle / \langle R_h \rangle$ as M_w increases has never been predicted or observed before, which should stimulate a theoretical study of uniform polymer clusters.

Conclusions

Introducing a small amount of 4-methacryloyloxy-2,2,6,6-tetramethylpiperidine-1-oxyl (MTEMPO) as branching agent can result in hyperbranched clusters which can undergo a reversible thermal decomposition at 100 °C or higher. The decomposition contains a three-stage process; namely, first from large clusters to smaller clusters without a significant change of the branching degree, then from smaller clusters to less

branched clusters, and finally from less branched clusters to short linear chains. The decomposition at 100 °C have a scaling of $\langle R_g \rangle / \langle R_h \rangle \propto M_w^{-0.20 \pm 0.01}$, revealing that even for a uniform cluster swollen in a good solvent, its periphery is more hydrodynamically draining.

Acknowledgment. Financial support of this work by The Special Funds for Major State Basic Research Projects (G1999064800), The NSFC Project (29974027), The CAS Bairen Project, and The RGC of the HKSAR Earmarked Grants (1999/00 CUHK 4209/99P, 2160122) is gratefully acknowledged.

References and Notes

- Hawker, C. J.; Frechet, J. M. J. *J. Am. Chem. Soc.* **1990**, *112*, 7638.
- Kim, Y. H.; Webster, O. W. *J. Am. Chem. Soc.* **1990**, *112*, 4592.
- Frechet, J. M. J. *Science* **1994**, *263*, 1710.
- Georges, M. K.; Veregin, R. P. N.; Kazmaier, P. M.; Hamer, G. K. *Macromolecules* **1993**, *26*, 2987.
- Veregin, R. P. N.; Georges, M. K.; Kazmaier, P. M. *Macromolecules* **1993**, *26*, 5316.
- Hawker, C. J. *J. Am. Chem. Soc.* **1994**, *116*, 11185.
- Yoshida, E. *J. Polym. Sci., Part A: Polym. Chem.* **1996**, *34*, 2937.
- Ottaviani, M. F.; Cossu, E.; Turro, N. J.; Tomalia, D. A. *J. Am. Chem. Soc.* **1995**, *117*, 7, 4387.
- Fukuda, T.; Terauchi, T.; Goto, A.; Tsujii, Y.; Miyamoto, T. *Macromolecules* **1996**, *26*, 3050.
- Leduc, M. R.; Hawker, C. J.; Dao, J.; Frechet, J. M. *J. Am. Chem. Soc.* **1996**, *118*, 10824.
- Hawker, C. J.; Graig, J. *Trends Polym. Sci.* **1996**, *4*, 183.
- Hussemann, M. H.; Malmstrom, E. E.; McNamara, M.; Mate, M.; Mecerreys, D.; Benoit, D. G.; Hedrick, J. L.; Mansky, P.; Huang, E.; Russell, T. P.; Hawker, C. J. *Macromolecules* **1999**, *32*, 1424.
- Li, C.; He, J.; Cao, J.; Yang, Y. *Macromolecules* **1999**, *32*, 7012.
- Aubert, C.; Cannell, D. S. *Phys. Rev. Lett.* **1986**, *56*, 738.
- Zhu, P. W.; Napper, D. H. *Phys. Rev. E* **1994**, *50*, 1360.
- Witten, T. A.; Sander, L. M. *Phys. Rev. Lett.* **1981**, *47*, 1400.
- Mandlbrot, B. *Fractal, Form and Dimensions*; Freeman: San Francisco, 1977.
- Nakata, M.; Nakagawa, T.; Nakamura, Y.; Wakatsuki, S. *J. Chem. Phys.* **1999**, *110*, 2711.
- Kurosaki, T.; Lee, K. W.; Okawara, M. *J. Polym. Sci., Polym. Chem.* **1972**, *10*, 3295.
- Miura, Y.; Hirota, K.; Moto, H.; Yamada, B. *Macromolecules* **1998**, *31*, 4659.
- Zhang, Y.; Xiang, M.; Jiang, M.; Wu, C. *Macromolecules* **1997**, *30*, 2035.
- Wang, X.; Qiu X.; Wu, C. *Macromolecules* **1998**, *31*, 2972.
- Chu, *Laser Light Scattering*, 2nd ed.; Academic Press: New York, 1991.
- Berne, B. J.; Pecora, R. *Dynamic Light Scattering*; Plenum Press: New York, 1976.
- Provencher, S. W. *Biophys. J.* **1976**, *16*, 27.
- Yamakawa, H. *Modern Theory of Polymer Solutions*; Harper and Row: New York, 1971.
- Murat, M.; Grest, G. S. *Macromolecules* **1996**, *29*, 1278.
- Weill, G.; des Cloizeaux, J. *J. Phys. (Paris)* **1979**, *40*, 99.

MA000569K